



Achieving superior ignition and combustion performance of Al/I₂O₅ biocidal nanoenergetic materials by CuO addition

Tao Wu^{a,*}, Erik Hagen^b, Haiyang Wang^b, Dylan J. Kline^c, Michael R. Zachariah^b, Carole Rossi^{a,*}

^a LAAS-CNRS, University of Toulouse, 7 Avenue du colonel Roche, Toulouse 31400s, France

^b University of California, Riverside, CA 92521, USA

^c University of Maryland, College Park, MD 20740, USA

ARTICLE INFO

Keywords:

Biocidal nanoenergetic materials
Iodine oxide
Copper oxide
Combustion
Reactivity
Synergetic effect

ABSTRACT

It was found that all iodine-containing biocidal energetic materials has a relatively long ignition delay upon combustion. A shorter ignition time (from the thermal trigger to the peak pressure) for Al/iodine oxides might further boost their combustion performance due to their high reactivity and high gas release rate. To achieve this goal, a secondary oxidizer, CuO, is incorporated into Al/I₂O₅ at different mass content keeping the overall thermite stoichiometry constant. The ternary Al/I₂O₅/CuO thermites were characterized in ignition using a T-jump ignition temperature set up, and in combustion in a constant volume combustion cell. Consequently, all ternary thermites outperform traditional Al/I₂O₅ counterpart with an optimum for 80/20 wt% of I₂O₅/CuO. This later composition ignites in 0.01 ms (30 times shorter than Al/I₂O₅) and produces peak pressure and pressurization rate of ~4 and 26 times greater than those produced by Al/I₂O₅. A series of additional characterizations using Fourier-transform infrared spectroscopy, Differential Scanning Calorimetry, Electrical/Thermal conductivity measurement, etc., permitted to unravel the cause of such improvement and to propose a reaction mechanism for this ternary Al/I₂O₅/CuO system. From an applications point of view, this study proposes a facile, inexpensive and efficient way to enhance the combustion performance of Al/I₂O₅ biocidal nanoenergetic materials.

1. Introduction

Anti-biological warfare agents with high-efficiency neutralization have gained increased attention due to an increasing threat of bioterrorism [1–5]. The current thinking is that an ideal neutralization process should generate not only a high temperature, but also release a long-lasting biocidal agent [6–9]. This is because a conventional energetic materials can result in low neutralization efficiency since they rely solely on a thermal neutralization pulse which is spatially distributed, may not provide enough thermal energy for long enough to kill the spores [10]. Therefore, it has been proposed that simultaneously delivering a rapid thermal pulse with a remnant biocidal agent would prolong the exposure time and improve the inactivation process [11]. Iodine-containing energetic materials have shown the most promise because of their excellent biocidal properties [12] compared to other biological energetic materials [13–15]. Different methods have been reported for incorporating elemental iodine into energetic materials [12,

16–18]. Dreizin et al. employed mechanically-alloyed aluminum-iodine composites as a fuel in energetic formulations and the initiation and combustion tests in air indicated that higher iodine concentration lowers initiation temperatures without substantially impacting the combustion temperatures [8]. They also found improvements in regards to pressurization rate and maximum pressure at constant volume with 15 wt.% and 20 wt.% of I₂. Wang et al. physically added iodine molecules into Al/CuO thermite and Al/PVDF systems, and found that the reaction rate was significantly decreased with increasing iodine content while a burn rate comparable to that of Al/PVDF film could be achieved with high iodine content (67 wt.%) when incorporated into a laminated structure [17,19].

Another efficient approach is to use iodine-containing oxy-compounds as an oxidizer - particularly iodine oxides and/or iodic acids. Among all the iodine oxides/iodic acids (I₂O₅, I₄O₉, HI₃O₈, HIO₃, H₅IO₆, etc. [20–22]), I₂O₅ is the most studied oxidizer in thermite systems [10, 23–26] due to its relatively high iodine content (~76 % iodine mass

* Corresponding authors.

E-mail addresses: twu@laas.fr (T. Wu), rossi@laas.fr (C. Rossi).

<https://doi.org/10.1016/j.combustflame.2023.113190>

Received 6 July 2023; Received in revised form 2 November 2023; Accepted 2 November 2023

Available online 18 November 2023

0010-2180/© 2023 The Combustion Institute. Published by Elsevier Inc. All rights reserved.

fraction) and high oxidizing power. In these studies, aluminum nanoparticles (nano-Al) with different sizes were chosen as the fuel due to its high reaction enthalpy, thermal conductivity and availability. With reported propagation velocities of up to $\sim 2000 \text{ m}\cdot\text{s}^{-1}$ for Al/I₂O₅ nanothermite [23], I₂O₅ shows a high potential in aluminum-based thermites as an extremely aggressive oxidizer. Constant volume combustion tests also show nano-Al/micro-I₂O₅ outperforms traditional aluminum-based thermites such as Al/micro-CuO and Al/micro-Fe₂O₃ [10]. A pre-ignition reaction is thought to trigger ignition in which ionic I₂O₅ fragments diffuse into the alumina-passivated shell, and create exothermic reactive complexes [25,27]. However, this mechanism is far from clear as Smith et al. reported that such pre-ignition reaction was not found for Al/nano crystalline I₂O₅ [28]. Wu et al. reported that aerosol-route synthesized iodine oxides/iodic acids outperform the corresponding commercial materials in combustion cell tests, where in particular Al/(aerosol-route synthesized) a-HI₃O₈ has the highest pressurization rate, highest peak pressure, and shortest burn time among all iodine-containing composites [29]. Later, Wu et al. employed carbon as an additive or main fuel into iodine oxides-based energetic materials and reported that carbon addition can lower initiation and iodine release temperatures due to a surface interaction between carbon and iodine oxide [30]. However, aluminum combined with iodine oxides/iodic acids shows long ignition delay ($\sim 0.3 \text{ ms}$) [29].

In this work, with the aim to increase the reactivity, i.e. shorten the ignition delay of 0.3 ms observed for all iodine oxides-based energetic, a strong oxidizer such as CuO [31–33] is added into the Al/I₂O₅ thermites at different mass ratio. I₂O₅ is chosen because it is relatively easy to prepare in comparison to other iodine oxides via aerosol spray pyrolysis [16,29], and is physically mixed with Al nanopowders. Ignition and combustion of the as-prepared ternary Al/I₂O₅/CuO thermites are characterized to determine the ignition delay, flame temperatures, pressure development in a constant-volume combustion cell. We find that the addition of CuO into Al/I₂O₅ thermites leads to a new promising biocidal nanoenergetic materials featuring reduced ignition delays ($\div 30$), shorter burn times ($\div 2$), higher combustion temperatures ($\sim 4650 \text{ }^\circ\text{C}$ against $\sim 3900 \text{ }^\circ\text{C}$). Further, additional experiments and analyses including thermal analysis permitted to conclude on a double positive effect of CuO on the Al/I₂O₅ thermite. Not only the CuO is a strong oxidizer with limited influence on the low temperature decomposition of I₂O₅ but also, CuO features a much higher thermal conductivity than I₂O₅, which could favor the thermal transport governing the reaction process. We also experimentally demonstrated that 20 wt% of CuO leads to the best ignition and combustion properties.

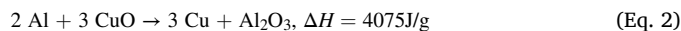
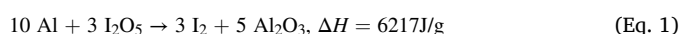
2. Experimental

2.1. Materials

The aluminum nanopowders (Al) (Alex, $\sim 80 \text{ nm}$) were purchased from Novacentrix. The active Al was 81 % by mass, determined by thermogravimetric analysis. Iodic acid and nanosized CuO ($\sim 100 \text{ nm}$) purchased from Sigma-Aldrich were directly used as received. All the other chemicals were of analytical grade and used as purchased without further treatment. I₂O₅ was prepared via aerosol spray pyrolysis with a silica gel regeneration temperature of $80 \text{ }^\circ\text{C}$ and a furnace temperature of $340 \text{ }^\circ\text{C}$ that is slightly different from the preparation method for a-I₂O₅ in our previous work [29].

2.2. Preparation of ternary thermites

Aluminum was stoichiometrically mixed with I₂O₅ and/or CuO based on the following equation in hexane followed by 30 min of sonication.



The detailed chemical constituents of thermites tested is summarized below in Table 1. After room temperature evaporation of the solvent in a desiccator, the solid thermite powders were used. The percentages in Al/I₂O₅/CuO_x% are referring to the molar percentage of aluminum that would be consumed by CuO (the far-right column in Table 1). Take sample Al/I₂O₅/CuO_20 % for example, 20 % of the aluminum would stoichiometrically react with CuO and the remaining 80 % of aluminum would react with I₂O₅. To simplify the following discussion regarding the ignition and combustion properties of different Al/I₂O₅/CuO_x% samples, we will refer to x% simply as CuO loading.

2.3. Chemical and thermal characterizations

Attenuated total reflection (ATR) FTIR spectra of the thermite powders were collected using a Nicolet iS-50R spectrometer equipped with a room temperature deuterated triglycine sulfate (DTGS) detector FTIR spectroscopy. A Thermo Scientific Smart iTX accessory was installed to collect the ATR spectra shown here at 4 cm^{-1} resolution and averaged over 30 scans. The thermal decomposition of the thermite powders was characterized under a ramping heating profile at $10 \text{ }^\circ\text{C}/\text{min}$ by a METTLER TOLEDO TGA 2 and a NETZSCH DSC 404 F3 Pegasus device equipped with a DSC—Cp sensor type S over a temperature ranging from ambient to $1000 \text{ }^\circ\text{C}$. Experiments were performed with $\sim 5 \text{ mg}$ of composites in platinum crucibles in (99.998 % pure) at a flow rate of $20 \text{ mL}/\text{min}$. The traces are normalized by the mass of energetic composite material.

2.4. Combustion tests

Combustion properties of thermites were evaluated in a constant-volume combustion cell, with simultaneous pressure and optical emission measurements. 25 mg of thermite powders was loosely loaded inside the cell (constant volume, $\sim 20 \text{ cm}^3$) and ignited by a resistively heated nichrome wire. The wire touches the top of the thermite powder and the reaction propagate downward upon ignition. The temporal pressure and optical emission from the thermite reaction were measured using a piezoelectric pressure sensor and a photodetector, respectively. By plotting the data as shown in Figure S1, pressurization rate, maximum pressure and burn time can be obtained and used for evaluation of the combustion performance. Pressurization rate is calculated by dividing the first peak pressure by the corresponding time. Burn time is defined as the full width of the half maximum of the optical profile. More detailed information on the combustion cell test can be found in our previous publications [29,34].

2.5. Ignition tests

The ignition of the thermite was investigated using a T-Jump as in several previous papers [35,36]. In brief, a $\sim 1 \text{ cm}$ long platinum wire ($76 \text{ } \mu\text{m}$ in width) with a thin layer coating of sample was rapidly joule-heated to about $1200 \text{ }^\circ\text{C}$ by a 3 ms pulse at a heating rate of $\sim 5 \times 10^5 \text{ }^\circ\text{C}\cdot\text{s}^{-1}$. A high-speed camera (Vision Research Phantom v12.0) was also employed to identify the point of initiation and burn time. The current and voltage signals were recorded, and the temporal temperature of the wire was measured according to the Callendar–Van Dusen equation [30,36]. Ignition delay of thermite reactions in T-jump experiments were defined and measured as the time of ignition where the first light is observed from high speed imaging of the whole combustion event. Then, applying the ignition delay in the temporal temperature curve of the wire, ignition temperatures of thermite reactions were measured. Each measurement was repeated at least 3 times.

Table 1
Chemical constituents of various thermites powders tested in this work ^a.

Thermites	Weight, mg				Weight percentage of CuO in oxidizers	Molar percentage of Al reacting with CuO
	Al	I ₂ O ₅	CuO	Total		
Al/I ₂ O ₅	6.3	18.7	—		0%	0%
Al/I ₂ O ₅ /CuO_20%	6.1	15.1	3.8	25.0	20%	20%
Al/I ₂ O ₅ /CuO_40%	5.9	11.1	8.0		42%	40%
Al/I ₂ O ₅ /CuO_60%	5.7	6.2	13.1		68%	60%
Al/I ₂ O ₅ /CuO_80%	5.6	3.5	15.9		80%	80%
Al/CuO	5.5	—	19.5		100%	100%

^a : Al active content is 81%; all thermites are prepared in the stoichiometric condition.

3. Results and discussion

3.1. Ternary Al/I₂O₅/CuO thermites outperforming Al/I₂O₅

Fig. 1 plots the temporal pressure profiles of Al/CuO and Al/I₂O₅, I₂O₅ being synthesized by aerosol-route [29] characterized in a constant volume combustion cell. We clearly see the ~0.3 ms ignition delay between the two pressure history profiles of the two thermites systems, as mentioned in the introduction. Since aerosol-route synthesized I₂O₅ have particles sizes of ~0.5 μm (spam from 0.1 to 1 μm), the ignition delay might be caused by the difference between the particle sizes of these two oxidizers [29]. However, the smallest size of I₂O₅ achievable remains larger than 0.5 μm [16,37] leaving a low possibility of testing nanosized I₂O₅ (< 100 nm, as individual nanoparticles rather than cluster).

This is the reason why we propose to incorporate nanosized CuO into the Al/I₂O₅ thermite powders varying the ratio between the two oxidizers while maintaining the same stoichiometric condition. They are referred as Al/I₂O₅/CuO_20 %, Al/I₂O₅/CuO_40 %, Al/I₂O₅/CuO_60 % and Al/I₂O₅/CuO_80 % (see Table 1 for more details). Fig. 2 presents their temporal pressure profiles obtained in the pressure cell and compared with Al/CuO and Al/I₂O₅ obtained in the same conditions to serve as reference. As expected, upon addition of CuO, the ignition delay disappeared. And, surprisingly, all four ternary systems significantly outperform the Al/I₂O₅ and Al/CuO in terms of the peak pressure whereas Al/CuO features smaller gas production (5.4 mmol.g⁻¹) in comparison with Al/I₂O₅ (6.3 mmol.g⁻¹) [38]. One would expect to obtain weakened combustion performance from the ternary systems when CuO is added to Al/I₂O₅.

A summary of the pressure development results is more easily digested in Fig. 3a-b confirming that addition of CuO increases the peak pressure and pressurization rate of Al/I₂O₅ even at small mass loadings of CuO. Evidently, Al/I₂O₅/CuO_20 %, gives the best performances: the ignition delay is reduced by almost 30 times as opposed to Al/I₂O₅ and pressure peak is increased by roughly 4 and 26 times, compared to Al/

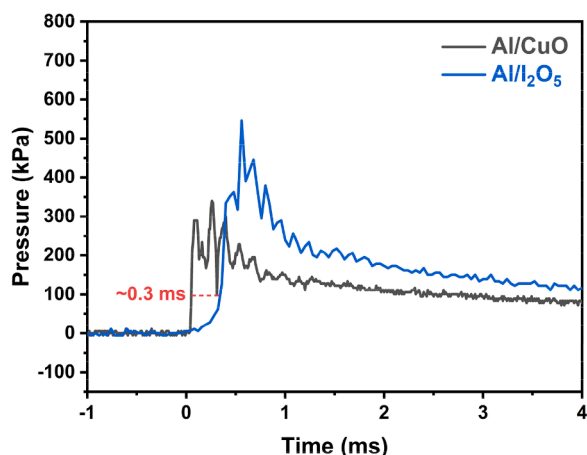


Fig. 1. Temporal pressure traces of Al/CuO and Al/I₂O₅.

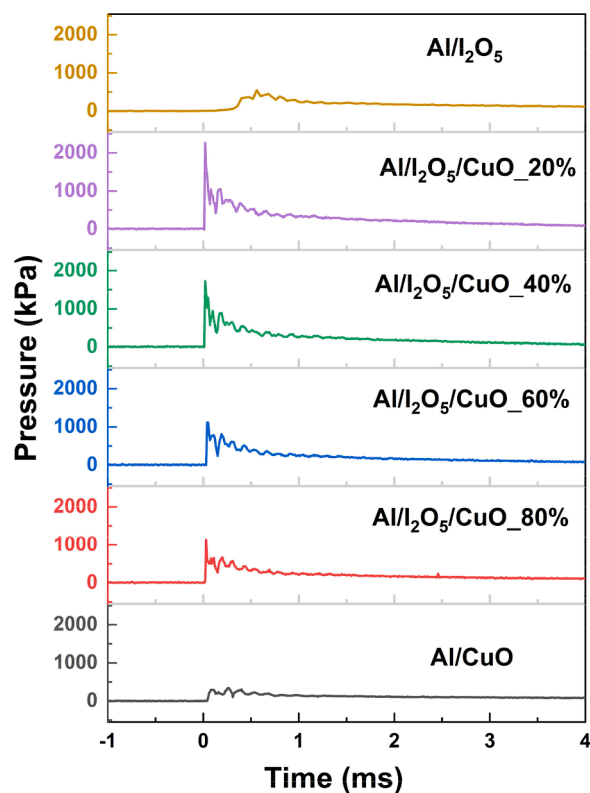


Fig. 2. Temporal pressure traces of different Al/I₂O₅/CuO thermite powders.

I₂O₅ and Al/CuO, respectively. With higher CuO loading, the improvement is not as important but is still better than the neat formulation of either oxidizer with Al.

The ignition temperature of all thermite powders characterized by T-Jump at a heating rate at $\sim 5 \times 10^5$ C.min⁻¹ and under vacuum is plotted in Fig. 3c. All ternary Al/I₂O₅/CuO thermites ignite at a temperature slightly lower than that of Al/I₂O₅. Again, Al/I₂O₅/CuO_20 % features the lowest ignition temperature, 540 °C.

Next, the average flame temperatures obtained by color ratio pyrometry following a previously published method [39] are plotted in Fig. 3d, along with the adiabatic temperature calculated using Cheetah. The typical snapshots and corresponding flame temperature map of Al/I₂O₅ are shown in Figure S2 as an example. Al/CuO thermite has the lowest flame temperature in accordance with Cheetah 5.0 [3] thermochemical code (considering a total mass of 25 mg in a 20 cm³vol). However, all four Al/I₂O₅/CuO ternary thermites have either similar or higher flame temperature than Al/I₂O₅. Al/I₂O₅/CuO_40 % and Al/I₂O₅/CuO_20 % thermites feature the maximum flame temperature (4650 °C), about 750 °C more than Al/I₂O₅ at 3900 °C. It has to be noted that for more than 40 % of CuO loading, the flame temperature decreases but remains hotter than those of Al/I₂O₅ indicating that Al/I₂O₅ succeed in maintaining a high temperature combustion regime even

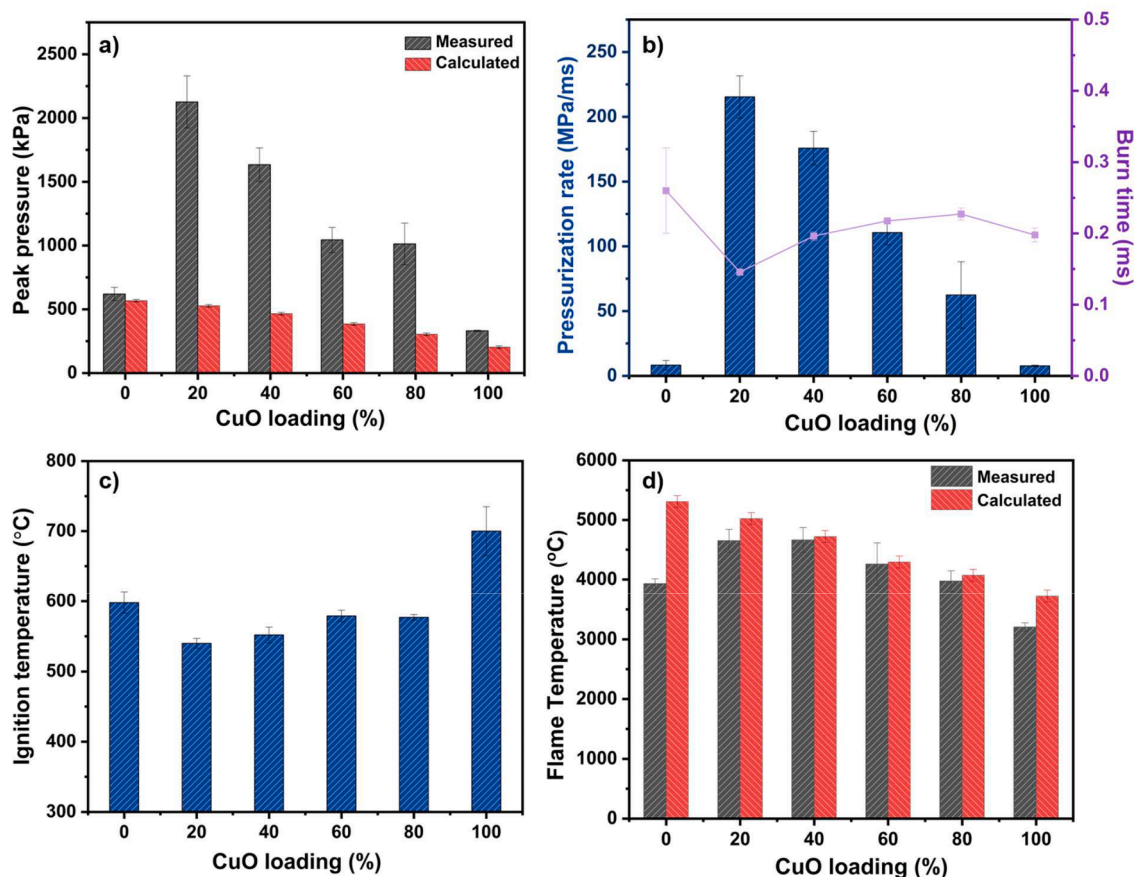


Fig. 3. Measured and calculated peak pressure (a), measured pressurization rate and burn time (b), ignition temperature (c), measured and calculated flame temperature (d), of Al/I₂O₅ with different CuO loading.

with only 20 % of I₂O₅ in the oxidizer. A more convincing result could be seen if we change the point of view to Al/CuO with I₂O₅ addition. The flame temperature of Al/CuO jumps from 3200 °C to 4000 °C when only 20 % of I₂O₅ is incorporated into the system, confirming that the dominant thermite reaction is governed between Al and I₂O₅ which generates more heat than that of Al and CuO. Interestingly, in Fig. 3d, whereas both binary thermite systems did not achieve their adiabatic flame temperatures probably due to incomplete reaction [39], all ternary systems feature flame temperatures much closer to their adiabatic temperature (<300 °C), the closest being obtained for

Al/I₂O₅/CuO₂₀ %.

As a summary of the ignition and combustion results, addition of a strong oxidizer such as CuO into Al/I₂O₅ thermites lead to promising new thermite composition featuring reduced ignition delays (÷ 30), shorter burn times (÷ 2), and higher combustion temperatures (4650 °C against 3900 °C). We speculate that these new ternary thermite couples benefit from the advantages of each oxidizers. CuO due to its strong facility to release its oxygen at temperature as low as 477 °C [35,40], may impact the ignition of the Al fuel in the ternary thermite and might be responsible for the observed lower ignition delays and shorter burn

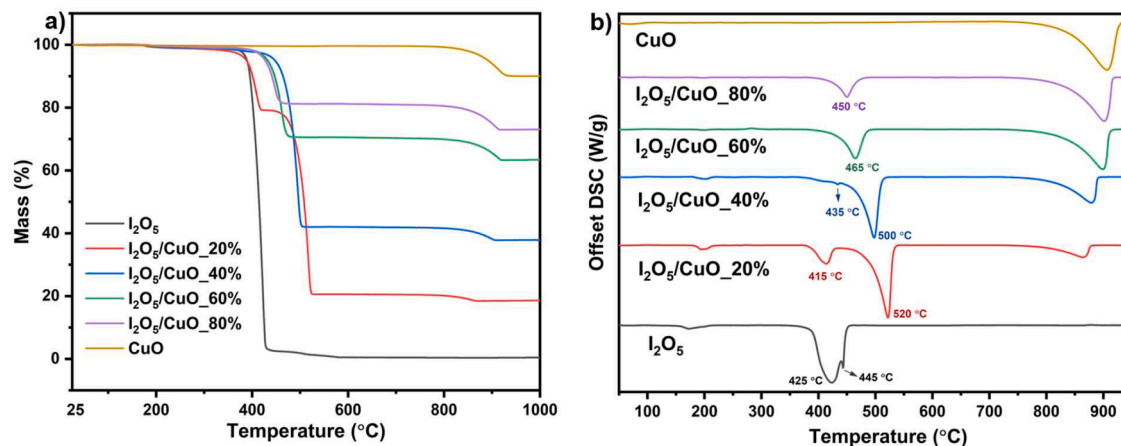


Fig. 4. TGA (a) and DSC (b) results of I₂O₅, I₂O₅/CuO₂₀ %, I₂O₅/CuO₄₀ %, I₂O₅/CuO₆₀ %, and I₂O₅/CuO₈₀ %. TGA/DSC experiments were performed in argon at a heating rate of 10 °C/min.

times. While I_2O_5 oxidizer decomposition into gaseous I_2 and O_2 below $400\text{ }^\circ\text{C}$ ensures a gas phase reaction producing high temperature combustion regime, i.e. above the vaporization of the products (Al_2O_3 , Cu, I_2 , etc.) and high-pressure development. To further investigate this speculation, we conduct two additional experiments. I_2O_5/CuO with different CuO loadings, and, then $Al/I_2O_5/CuO$ thermites were analyzed by TGA/DSC at a heating rate of $10\text{ }^\circ\text{C}\cdot\text{min}^{-1}$ in Ar (Fig. 4) with the goal to: (1) quantify the influence of CuO content on the I_2O_5 decomposition process and onset; and, (2) quantify the influence of CuO on the nature of the low temperature exothermic events. For comparison, same experiments were conducted on Al/I_2O_5 and Al/CuO powders.

3.2. Influence of CuO on I_2O_5 decomposition

The I_2O_5 decomposition undergoes the following two stages (black curves in TGA and DSC curves in Fig. 4): a nearly negligible minor endothermic event located at around $200\text{ }^\circ\text{C}$ corresponds to dehydration of HI_3O_8 (a rehydrated product of I_2O_5 during preparation process due to its high hygroscopicity); the main endothermic event starting at $370\text{ }^\circ\text{C}$ corresponds to the complete decomposition of I_2O_5 into gaseous I_2 and O_2 . A small shoulder peak is spotted at around $450\text{ }^\circ\text{C}$ along with the major endothermic peak in its DSC result. While, the TGA curve of I_2O_5 indicates its complete decomposition in one step with an onset decomposition temperature at $\sim 370\text{ }^\circ\text{C}$.

Both TGA and DSC results show that the CuO addition has nearly no influence on the first decomposition step of I_2O_5 but rather pose significant impacts on the second endothermic event spanning from 350 to $550\text{ }^\circ\text{C}$ based on the amount of CuO loading. With 20% CuO loading, the decomposition temperature of I_2O_5 slightly decreases to $360\text{ }^\circ\text{C}$ (red curve in Fig. 4a), indicating a beneficial effect on the decomposition of I_2O_5 . But the decomposition pauses at $420\text{ }^\circ\text{C}$ and resumes again at $460\text{ }^\circ\text{C}$ and finishes at $525\text{ }^\circ\text{C}$. The DSC result (red curve in Fig. 4b) shows that the peak at $425\text{ }^\circ\text{C}$ from neat I_2O_5 shifted to a lower temperature at $415\text{ }^\circ\text{C}$; meanwhile the shoulder peak at $445\text{ }^\circ\text{C}$ from bare I_2O_5 shifted to $520\text{ }^\circ\text{C}$ and separated from the main peak to appear as a single endothermic peak making the decomposition of I_2O_5 into three steps. A similar phenomenon was also found previously by Pantoya et al. [25] where an extra endotherm with a peak temperature at $\sim 510\text{ }^\circ\text{C}$ emerged after mixing Al_2O_3 and I_2O_5 together (with $\sim 20\text{ wt}\%$ Al_2O_3 loading). They claimed that the exothermic binding process between the released gasses and Al_2O_3 brings the heat flow curve back to its baseline. Then upon the Al_2O_3 phase change from amorphous to γ with an onset at $\sim 480\text{ }^\circ\text{C}$, the absorbed I_2 and O_2 gasses by Al_2O_3 starts desorption and results in the emergence of the third endothermic event. It appears that CuO is functioning very similarly as Al_2O_3 towards the decomposition behavior of I_2O_5 here by separating its second decomposition step into two stages.

While 20% addition of CuO demonstrates weak positive influence on decomposition of I_2O_5 by reducing its onset decomposition temperature by only $10\text{ }^\circ\text{C}$, higher CuO loadings on the contrary pose negative impact by increasing the I_2O_5 onset decomposition temperature from $370\text{ }^\circ\text{C}$ to temperatures higher than $420\text{ }^\circ\text{C}$ as shown in Fig. 4a and Table 2. The DSC results (Fig. 4b) also show that the endothermic peak at $425\text{ }^\circ\text{C}$ from neat I_2O_5 moves to higher temperatures when CuO addition is more than

Table 2

Onset decomposition temperatures of the I_2O_5 decomposition from TGA experiments of I_2O_5 , $I_2O_5/CuO_{20\%}$, $I_2O_5/CuO_{40\%}$, $I_2O_5/CuO_{60\%}$, and $I_2O_5/CuO_{80\%}$.

	Onset decomposition temperature ($^\circ\text{C}$)
Al/I_2O_5	370
$I_2O_5/CuO_{20\%}$	360
$I_2O_5/CuO_{40\%}$	430
$I_2O_5/CuO_{60\%}$	420
$I_2O_5/CuO_{80\%}$	420

20%. It appears that only a small portion of CuO can facilitate the decomposition of I_2O_5 and in fact excess CuO even slows down I_2O_5 decomposition. Such results explain why $Al/I_2O_5/CuO_{20\%}$ exhibits the best ignition performance than the other ternary systems (Fig. 3); however, it still does not account for the significant enhancement of Al/I_2O_5 combustion when CuO is added.

As addition of CuO into I_2O_5 leads to a slight increase in the I_2O_5 decomposition onset (except at 20% loading), it is not possible to explain the low ignition delay and faster burn rate of $Al/I_2O_5/CuO$ thermites by considering only chemical and physical transformations. Next, we quantify the influence of CuO on the nature of the low temperature exothermic events of the ternary systems. For comparison, same experiments were conducted on Al/I_2O_5 reference thermite.

3.3. Influence of CuO on Al/I_2O_5 low temperature reactions

Different from the two-stepped decomposition of I_2O_5 , the DSC curve of Al/I_2O_5 features a more complex pathway as shown in Fig. 5 (blue curve) due to the exothermic redox reactions. Begins with a small endotherm at $\sim 200\text{ }^\circ\text{C}$ corresponding to the dehydration of HI_3O_8 similar to I_2O_5 . Then a major exothermic event with an onset temperature at $\sim 300\text{ }^\circ\text{C}$ caused by the oxidation of aluminum by oxygen from I_2O_5 . A previous study [41] has demonstrated that annealing aluminum-based thermites at temperatures $> 200\text{ }^\circ\text{C}$ could trigger modification of the $Al/oxidizer$ interface chemistry that shorten the diffusion length between aluminum core and oxidizers and thus facilitate the ignition process, which might explain the low onset temperature of the first exothermic Al/I_2O_5 reaction. Then the oxidation of aluminum event slows down by the endothermic event corresponds to the major decomposition of I_2O_5 , which peaked at a slightly lower temperature than neat I_2O_5 . With more I_2O_5 decomposition, the exothermic oxidation of aluminum continues and mark its DSC curve with multiple exothermic peaks spanned from 400 to $600\text{ }^\circ\text{C}$. And the third decomposition peak of I_2O_5 caused by the interaction between alumina and decomposition products I_2 and O_2 gasses is also present in the case of Al/I_2O_5 . Then the melting event of unreacted aluminum indicates the incomplete oxidization of aluminum.

Looking into the ternary systems, the top four curves in Fig. 5, it seems that they all appear to undergo similar thermal events except for $Al/I_2O_5/CuO_{20\%}$ case. The first exothermic event of $Al/I_2O_5/CuO_{20\%}$ has the same onset temperature ($\sim 300\text{ }^\circ\text{C}$) as Al/I_2O_5 ; however, such temperature increases gradually with higher CuO loading and reached a plateau at 40% CuO loading ($330\text{ }^\circ\text{C}$). When there is more than 40% of CuO loading in the ternary system, the onset of the Al/I_2O_5 reaction is slightly delayed to a higher temperature at low heating rate condition. In

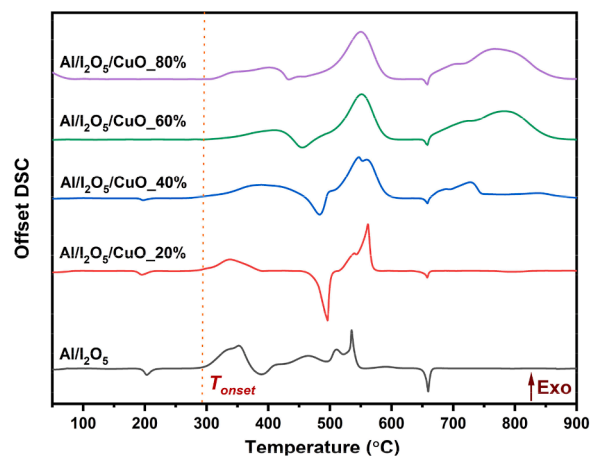


Fig. 5. DSC results of I_2O_5 , $I_2O_5/CuO_{3\%}$, Al/I_2O_5 , and $Al/I_2O_5/CuO$ ternary systems. DSC experiments were performed in argon at a heating rate of $10\text{ }^\circ\text{C}\cdot\text{min}^{-1}$.

addition, no more exothermic event is found after 600 °C for the case of Al/I₂O₅/CuO_20 %, indicating that the thermal activities of Al/I₂O₅/CuO_20 % finishes within a much smaller temperature range than the other systems in this work. Therefore, at low heating rate, Al/I₂O₅/CuO_20 % features equivalent onset temperature and shorter reaction duration in comparison to Al/I₂O₅ redox reaction.

DSC analyses of ternary thermites confirms that the incorporation of 20 % of CuO into Al/I₂O₅ provokes a slight decrease in the I₂O₅ decomposition onset and more complete reaction, but they fail in disclosing the mechanisms at the origin of this reduced ignition delay. Can it be caused by a catalytic effect provoked by chemical interactions between the two oxides? I₂O₅/CuO physically mixed oxides were examined by FTIR (Figure S3) and no noticeable change of the CuO and I₂O₅ spectra were found which confirms that no chemical interaction occurs between the two oxidizers at ambient. Last likely cause of the very short ignition delay is a modification of the thermal properties of the thermite mixture when adding CuO into the Al/I₂O₅.

3.4. Discussion on the role of thermal properties on the ignition delay

The ignition of the ternary thermite is performed by Joule heating as loose powders “enrobe” a thin Nichrome wire. In this heating configuration, evidently, the thermal properties of the thermite material play a critical role in the diffusion of the heat from the hot wire to the thermite. This can explain the difference in the ignition delay between Al/I₂O₅ and Al/CuO. The material with higher thermal conductivity will show a shorter ignition delay [42]. The thermal conductivity of nanosized CuO is ~30 W.m⁻¹.k⁻¹ [43,44]. Unfortunately, such data is not available for I₂O₅ in the literature. Thus, as - according to Wiedemann–Franz law - the thermal conductivity is positively correlated to the electrical conductivity, we propose to make an evaluation of thermal conductivity trend between I₂O₅ to CuO oxidizer based on the electrical properties. Both oxides were pressed into coin pellets (~0.5 mm in thickness) before resistivity measurement. At the ambient, the sheet resistance of CuO is measured at ~550 kΩ/□; where I₂O₅ has a sheet resistance even exceeds the tool range to be gauged; i.e., CuO is a much better electrical conductor than I₂O₅. So that we can deduce that CuO is a better thermal conductor than I₂O₅. Hence, replacing some I₂O₅ oxide by CuO improves the overall powder thermal conductivity and helps thermal transfer from the hot wire and within the thermites. This simple reasoning helps us to understand why ternary thermite has a shorter ignition delay and shorter burn time as well. This was verified by a last experiment: 20 %, 40 %, and 60 % addition of Ag₂O particles having the same dimension as CuO particles and featuring a slightly lower thermal conductivity (~25 W.m⁻¹.k⁻¹) [45] is added to Al/I₂O₅ thermite and tested in ignition and combustion under the same conditions. As shown in Fig. 6, Ag₂O addition shows almost the same effect as CuO addition on ignition delay and

burn time, increasing peak pressure and pressurization rate, and meanwhile maintaining the high flame temperature of Al/I₂O₅, except for the scale of the enhancements by Ag₂O addition is much weaker than the case of CuO. It makes sense since Ag₂O is a much weaker oxide than CuO in aluminum-based thermites based on previous reported work [46–48]. Thus, it is reasonable to assume that adding a secondary metal oxide that features a good thermal conductivity into Al/I₂O₅ thermite can extensively boost its overall combustion performance in a constant volume combustion cell.

3.5. Reaction mechanisms of Al/I₂O₅/CuO

From all aforementioned characterization results and analyses we can propose a reaction mechanism of Al/I₂O₅/CuO (Fig. 7). Al/CuO ignites readily upon triggering by Joule heating. The generated heat/energy then ignites the adjacent Al/I₂O₅. The high reaction temperature from Al/I₂O₅ facilitates the further decomposition of the remaining oxidizers, which in turn accelerates the aluminum oxidation by providing large amount of oxygen and leads to a shorter burn time. Thus, the additive CuO shortens the ignition delay of Al/I₂O₅ but also -being a strong oxidizer- release a high amount of gaseous oxygen for aluminum to react. In parallel, the very high flame temperature of the Al/I₂O₅ reaction occurring in gaseous phase further boosts the pressure. High temperature and high oxygen content result in a shortened pressure pulse of high amplitude and rate accelerate the overall reaction. All those events occur simultaneously within 0.15 ms, so that we can conclude as a synergistic effect of both oxidizers which enhances the ignition and combustion performance of Al/I₂O₅ in a closed volume environment.

4. Conclusions

A secondary oxidizer CuO was incorporated into Al/I₂O₅ system with the goal to shorten its ignition delay without penalizing their combustion performance (pressure development). Four different Al/I₂O₅/CuO thermites with varying oxidizer mass ratios were characterized in ignition and combustion in a constant volume combustion cell. The four ternary thermites all feature higher peak pressures, pressurization rates, flame temperatures and shorter ignition delay than that of Al/I₂O₅. Multiple characterization tools were used to identify the cause of such improvement. FTIR analysis show no surface interaction between the two oxides. TGA/DSC results show that CuO addition has limited influence on the decomposition of I₂O₅ and on the reaction of Al/I₂O₅. However, it has been verified in this work that CuO has a much better thermal conductivity than I₂O₅, which improves the thermal transfer within the Al/I₂O₅/CuO thermites and thus creates a positive effect on its combustion. Finally, a reaction mechanism could be proposed for Al/

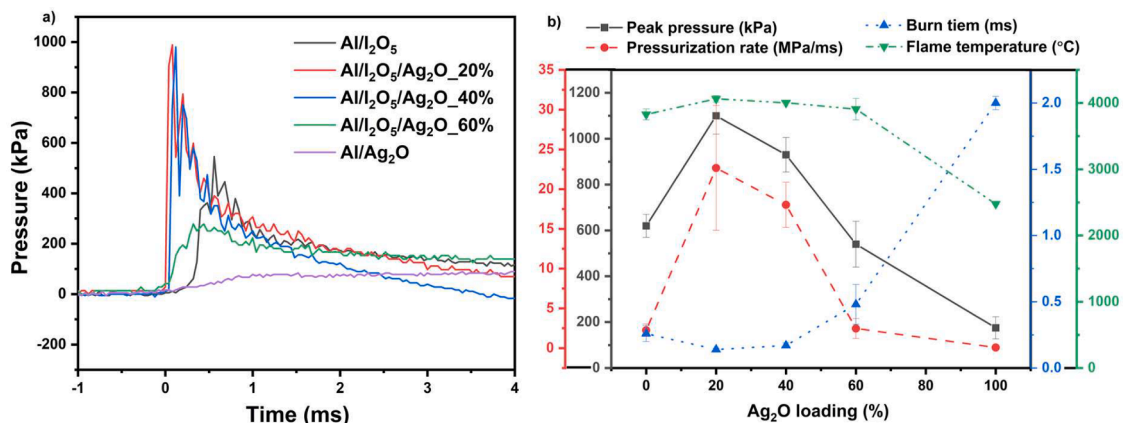


Fig. 6. Temporal pressure traces (a) and combustion performance (b) of different Al/I₂O₅/Ag₂O thermites.

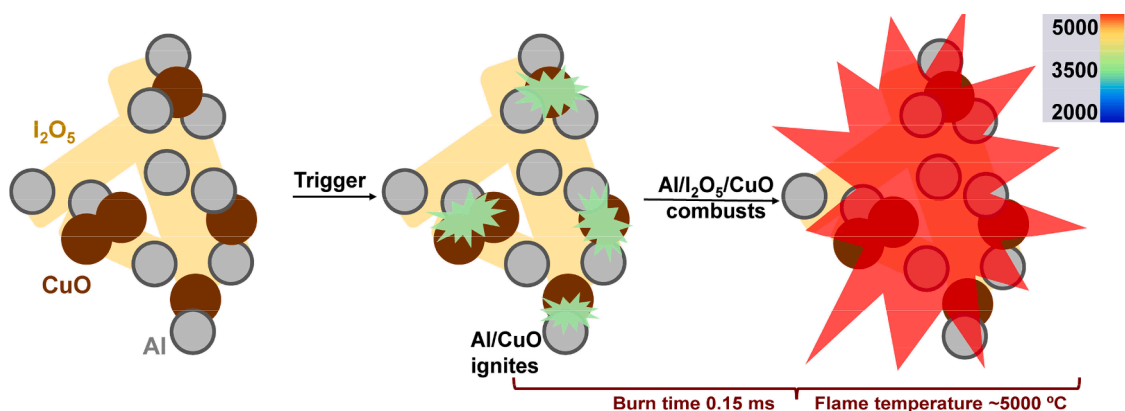


Fig. 7. Schematics of the boosting mechanism of Al/I₂O₅ combustion by CuO addition.

I₂O₅/CuO to explain this unexpected improvement. This work not only proposed a new high performing biocidal energetic material containing 80/20 wt% of I₂O₅/CuO but also unravel the reasons of ignition and combustion performances enhancement for potential applications.

Novelty and significance statement

we incorporated a secondary oxidizer CuO into Al/I₂O₅ system with the goal to shorten its ignition delay without penalizing their combustion performance (pressure development). Surprisingly the CuO addition not only eliminated the ignition delay of Al/I₂O₅ in a constant-volume combustion cell but also demonstrated significant enhancement on peak pressures, pressurization rates, flame temperatures and shorter ignition delay compared to that of either Al/CuO or Al/I₂O₅. Multiple characterization tools were used to identify the cause of such improvement. Then we verified that CuO has a much better thermal conductivity than I₂O₅, which improves the thermal transfer within the Al/I₂O₅/CuO thermites and thus creates a positive effect on its combustion. This work not only proposed a new high performing biocidal energetic material containing 80/20 wt% of I₂O₅/CuO but also elucidate the reasons of enhancement on ignition and combustion performance.

Authors contributions

T.W. conceived the idea, designed and carried out the present work. T.W., M.R.Z., and C.R. wrote the paper. E.H. and D.J.K. carried out calculations on constant-volume thermite combustion. H.W. and D.J.K. assisted T.W. in combustion cell test and flame temperature measurement. M.R.Z. and C.R. supervised this research.

Appendix A. Supplementary data

Supplementary data to this article can be found online at <https://>

Declaration of Competing Interest

The authors declare that they have no known competing financial interests or personal relationships that could have appeared to influence the work reported in this paper.

Acknowledgement

This work was supported by the European Research Council (H2020 Excellent Science) Researcher Award (grant 832889 –PyroSafe) and the DTRA on Materials Science in Extreme Environments. The authors acknowledge the help from Dr. Yuteng Zhang (Le laboratoire de chimie de coordination, LCC) and Dr. Sylvain Pelloquin (LAAS) for electrical property measurement.

Supplementary materials

Supplementary material associated with this article can be found, in the online version, at [doi:10.1016/j.combustflame.2023.113190](https://doi.org/10.1016/j.combustflame.2023.113190).

References

- [1] Meeusen Blatchley, Aronson Anne, I. Arthur, Lindsay Brewster, Inactivation of bacillus spores by ultraviolet or gamma radiation, *J. Environ. Eng.* 131 (2005) 1245–1252, [https://doi.org/10.1061/\(ASCE\)0733-9372\(2005\)131_9\(1245\)](https://doi.org/10.1061/(ASCE)0733-9372(2005)131_9(1245)).
- [2] M. Schoenitz, T.S. Ward, E.L. Dreizin, Fully dense nano-composite energetic powders prepared by arrested reactive milling, *Proc. Combust. Inst.* 30 (2005) 2071–2078, <https://doi.org/10.1016/j.proci.2004.08.134>.
- [3] W. Zhao, X. Wang, H. Wang, T. Wu, D.J. Kline, M. Rehwoldt, H. Ren, M. R. Zachariah, Titanium enhanced ignition and combustion of Al/I₂O₅ mesoparticle composites, *Combust. Flame.* 212 (2020) 245–251, <https://doi.org/10.1016/j.combustflame.2019.04.049>.
- [4] L.N. Kotter, L.J. Groven, Boron carbide based biocide compositions: a study of iodate particle size on combustion and iodine output, *Propellants Explos. Pyrotech.* 45 (2020) 509–516, <https://doi.org/10.1002/prep.201900278>.
- [5] T. Wu, F. Sevely, B. Julien, F. Sodre, J. Cure, C. Tenailleau, A. Esteve, C. Rossi, New coordination complexes-based gas-generating energetic composites, *Combust. Flame.* 219 (2020) 478–487, <https://doi.org/10.1016/j.combustflame.2020.05.022>.
- [6] K.T. Sullivan, N.W. Piekielek, S. Chowdhury, C. Wu, M.R. Zachariah, C.E. Johnson, Ignition and combustion characteristics of nanoscale Al/AgI₃: a potential energetic biocidal system, *Combust. Sci. Technol.* 183 (2010) 285–302, <https://doi.org/10.1080/00102202.2010.496378>.
- [7] S. Zhang, M. Schoenitz, E.L. Dreizin, Mechanically alloyed Al–I composite materials, *J. Phys. Chem. Solids.* 71 (2010) 1213–1220, <https://doi.org/10.1016/j.jpcs.2010.04.018>.
- [8] S. Zhang, C. Badiola, M. Schoenitz, E.L. Dreizin, Oxidation, ignition, and combustion of AlI₂ composite powders, *Combust. Flame.* 159 (2012) 1980–1986, <https://doi.org/10.1016/j.combustflame.2012.01.004>.
- [9] F.T. Tabit, E. Buys, The effects of wet heat treatment on the structural and chemical components of *Bacillus sporothermodurans* spores, *Int. J. Food Microbiol.* 140 (2010) 207–213, <https://doi.org/10.1016/j.ijfoodmicro.2010.03.033>.
- [10] G. Jian, S. Chowdhury, J. Feng, M.R. Zachariah, The ignition and combustion study of nano-al and iodine pentoxide thermite, 8th US Natl. Combust. Meet. 2013. 2 (2013) 1287–1299.
- [11] H. Wang, G. Jian, W. Zhou, J.B. DeLisio, V.T. Lee, M.R. Zachariah, Metal iodate-based energetic composites and their combustion and biocidal performance, *ACS Appl. Mater. Interfaces* 7 (2015) 17363–17370, <https://doi.org/10.1021/acsami.5b04589>.
- [12] Y. Aly, S. Zhang, M. Schoenitz, V.K. Hoffmann, E.L. Dreizin, M. Yermakov, R. Indugula, S.A. Grinshpun, Iodine-containing aluminum-based fuels for inactivation of bioaerosols, *Combust. Flame* 161 (2014) 303–310, <https://doi.org/10.1016/j.combustflame.2013.07.017>.
- [13] C.E. Johnson, K.T. Higa, Iodine-rich biocidal reactive materials, *MRS Online Proc. Libr.* 1521 (2013) 307, <https://doi.org/10.1557/opl.2013.46>.
- [14] O. Mulamba, E.M. Hunt, M.L. Pantoya, Neutralizing bacterial spores using halogenated energetic reactions, *Biotechnol. Bioprocess Eng.* 18 (2013) 918–925, <https://doi.org/10.1007/s12257-013-0323-3>.
- [15] C. He, J. Zhang, J.M. Shreeve, Dense iodine-rich compounds with low detonation pressures as biocidal agents, *Chem. Eur. J.* 19 (2013) 7503–7509, <https://doi.org/10.1002/chem.201300565>.
- [16] T. Wu, A. SyBing, X. Wang, M.R. Zachariah, Aerosol synthesis of phase pure iodine/iodic biocidal microparticles, *J. Mater. Res.* 32 (2017) 890–896, <https://doi.org/10.1557/jmr.2017.6>.
- [17] H. Wang, J.B. DeLisio, G. Jian, W. Zhou, M.R. Zachariah, Electrospray formation and combustion characteristics of iodine-containing Al/CuO nanothermite

- microparticles, *Combust. Flame* 162 (2015) 2823–2829, <https://doi.org/10.1016/j.combustflame.2015.04.005>.
- [18] S.E. Guerrero, E.L. Dreizin, E. Shafirovich, Combustion of thermite mixtures based on mechanically alloyed aluminum–iodine material, *Combust. Flame* 164 (2016) 164–166, <https://doi.org/10.1016/j.combustflame.2015.11.014>.
- [19] H. Wang, S. Holdren, M.R. Zachariah, Preparation and combustion of laminated iodine containing aluminum/polyvinylidene fluoride composites, *Combust. Flame* 197 (2018) 120–126, <https://doi.org/10.1016/j.combustflame.2018.05.016>.
- [20] B.K. Little, S.B. Emery, J.C. Nittinger, R.C. Fantasia, C.M. Lindsay, Physicochemical characterization of iodine(v) oxide, part 1: hydration rates, *Propellants Explos. Pyrotech.* 40 (2015) 595–603, <https://doi.org/10.1002/prop.201400225>.
- [21] A.I. Fischer, Redetermination of HI_3O_8 , an adduct of formula HIO_3 center dot I_2O_5 , *Acta Crystallogr. Sect. E-Struct. Rep. Online* (2005) 61.
- [22] A. Wikjord, P. Taylor, D. Torgerson, L. Hachkowski, Thermal behaviour of corona-precipitated iodine oxides, *Thermochim. Acta*. 36 (1980) 367–375, [https://doi.org/10.1016/0040-6031\(80\)87032-8](https://doi.org/10.1016/0040-6031(80)87032-8).
- [23] K.S. Martirosyan, Nanoenergetic gas-generators: principles and applications, *J. Mater. Chem.* 21 (2011) 9400–9405, <https://doi.org/10.1039/C1JM11300C>.
- [24] B.K. Little, E.J. Welle, S.B. Emery, M.B. Bogle, V.L. Ashley, A.M. Schrand, C. M. Lindsay, Chemical dynamics of nano-aluminum/iodine, *J. Phys. Conf. Ser.* 500 (2014), 052025, <https://doi.org/10.1088/1742-6596/500/5/052025>.
- [25] C. Farley, M. Pantoya, Reaction kinetics of nanometric aluminum and iodine pentoxide, *J. Therm. Anal. Calorim.* 102 (2010) 609–613, <https://doi.org/10.1007/s10973-010-0915-5>.
- [26] E.L. Dreizin, M. Schoenitz, Correlating ignition mechanisms of aluminum-based reactive materials with thermoanalytical measurements, *Prog. Energy Combust. Sci.* 50 (2015) 81–105, <https://doi.org/10.1016/j.pecs.2015.06.001>.
- [27] O. Mulamba, M.L. Pantoya, Exothermic surface chemistry on aluminum particles promoting reactivity, *Appl. Surf. Sci.* 315 (2014) 90–94, <https://doi.org/10.1016/j.apsusc.2014.07.112>.
- [28] D.K. Smith, K. Hill, M.L. Pantoya, J.S. Parkey, M. Kesmez, Reactive characterization of anhydrous iodine oxide (I_2O_5) with aluminum: amorphous versus crystalline microstructures, *Thermochim. Acta*. 641 (2016) 55–62, <https://doi.org/10.1016/j.tca.2016.08.013>.
- [29] T. Wu, X. Wang, P.Y. Zavalij, J.B. DeLisio, H. Wang, M.R. Zachariah, Performance of iodine oxides/iodic acids as oxidizers in thermite systems, *Combust. Flame* 191 (2018) 335–342, <https://doi.org/10.1016/j.combustflame.2018.01.017>.
- [30] T. Wu, X. Wang, J.B. DeLisio, S. Holdren, M.R. Zachariah, Carbon addition lowers initiation and iodine release temperatures from iodine oxide-based biocidal energetic materials, *Carbon*. 130 (2018) 410–415, <https://doi.org/10.1016/j.carbon.2018.01.001>.
- [31] C. Rossi, Engineering of Al/CuO reactive multilayer thin films for tunable initiation and actuation, *Propellants Explos. Pyrotech.* 44 (2019) 94–108, <https://doi.org/10.1002/prop.201800045>.
- [32] H. Jabraoui, M. Djafari Rouhani, C. Rossi, A. Esteve, First-principles investigation of CuO decomposition and its transformation into $\{\text{Cu}\}_2\{\text{O}\}$, *Phys. Rev. Mater.* 6 (2022), 096001 <https://doi.org/10.1103/PhysRevMaterials.6.096001>.
- [33] V. Baijot, L. Glavier, J.M. Ducéré, M. DjafariRouhani, C. Rossi, A. Estève, Modeling the pressure generation in aluminum-based thermites, *Propellants Explos. Pyrotech.* 40 (2015) 402–412, <https://doi.org/10.1002/prop.201400297>.
- [34] K. Sullivan, M. Zachariah, Simultaneous pressure and optical measurements of nanoaluminum thermites: investigating the reaction mechanism, *J. Propuls. Power.* 26 (2010) 467–472, <https://doi.org/10.2514/1.45834>.
- [35] J.B. DeLisio, X. Wang, T. Wu, G.C. Egan, R.J. Jacob, M.R. Zachariah, Investigating the oxidation mechanism of tantalum nanoparticles at high heating rates, *J. Appl. Phys.* 122 (2017), 245901, <https://doi.org/10.1063/1.4995574>.
- [36] G. Jian, N.W. Piekielek, M.R. Zachariah, Time-resolved mass spectrometry of nano-Al and nano-Al/CuO thermite under rapid heating: a mechanistic study, *J. Phys. Chem. C*. 116 (2012) 26881–26887, <https://doi.org/10.1021/jp306717m>.
- [37] F. Xu, P. Biswas, G. Nava, J. Schwan, D.J. Kline, M.C. Rehwoldt, L. Mangolini, M. R. Zachariah, Tuning the reactivity and energy release rate of I_2O_5 based ternary thermite systems, *Combust. Flame*. 228 (2021) 210–217, <https://doi.org/10.1016/j.combustflame.2020.12.047>.
- [38] S.H. Fischer, M. Grubelich, Theoretical Energy Release of Thermites, Intermetallics, and Combustible Metals, 1999.
- [39] R.J. Jacob, D.J. Kline, M.R. Zachariah, High speed 2-dimensional temperature measurements of nanothermite composites: probing thermal vs. Gas generation effects, *J. Appl. Phys.* 123 (2018), 115902, <https://doi.org/10.1063/1.5021890>.
- [40] H. Jabraoui, A. Esteve, M. Schoenitz, E.L. Dreizin, C. Rossi, Atomic scale insights into the first reaction stages prior to Al/CuO nanothermite ignition: influence of porosity, *ACS Appl. Mater. Interfaces*. 14 (2022) 29451–29461, <https://doi.org/10.1021/acsmi.2c07069>.
- [41] T. Wu, G. Lahiner, C. Tenaillieu, B. Reig, T. Hungria, A. Esteve, C. Rossi, Unexpected enhanced reactivity of aluminized nanothermites by accelerated aging, *Chem. Eng. J.* (2021), 129432, <https://doi.org/10.1016/j.cej.2021.129432>.
- [42] G. Lahiner, A. Nicollet, J. Zapata, L. Marín, N. Richard, M.D. Rouhani, C. Rossi, A. Estève, A diffusion–reaction scheme for modeling ignition and self-propagating reactions in Al/CuO multilayered thin films, *J. Appl. Phys.* 122 (2017), 155105, <https://doi.org/10.1063/1.5000312>.
- [43] A.A. Abdelmalik, A. Sadiq, Thermal and electrical characterization of composite metal oxides particles from periwinkle shell for dielectric application, *SN Appl. Sci.* 1 (2019) 373, <https://doi.org/10.1007/s42452-019-0388-5>.
- [44] H. Wang, B. Julien, D.J. Kline, Z. Alibay, M.C. Rehwoldt, C. Rossi, M.R. Zachariah, Probing the reaction zone of nanolaminates at $\sim\mu\text{s}$ time and $\sim\mu\text{m}$ spatial resolution, *J. Phys. Chem. C*. 124 (2020) 13679–13687, <https://doi.org/10.1021/acs.jpcc.0c01647>.
- [45] Y. Mou, J. Liu, Q. Wang, Z. Lei, Y. Peng, M. Chen, A novel thermal conductive Ag_2O paste for thermal management of light-emitting diode, *Mater. Lett.* 316 (2022), 132022, <https://doi.org/10.1016/j.matlet.2022.132022>.
- [46] T. Wu, M.R. Zachariah, Silver ferrite: a superior oxidizer for thermite-driven biocidal nanoenergetic materials, *RSC Adv.* 9 (2019) 1831–1840, <https://doi.org/10.1039/C8RA08997C>.
- [47] K.T. Sullivan, C. Wu, N.W. Piekielek, K. Gaskell, M.R. Zachariah, Synthesis and reactivity of nano- Ag_2O as an oxidizer for energetic systems yielding antimicrobial products, *Combust. Flame* 160 (2013) 438–446, <https://doi.org/10.1016/j.combustflame.2012.09.011>.
- [48] R. Russell, S. Bless, M. Pantoya, Impact-driven thermite reactions with iodine pentoxide and silver oxide, *J. Energ. Mater.* 29 (2011) 175–192, <https://doi.org/10.1080/07370652.2010.514318>.